Design and application of an instrumented projectile for load measurements during impact

Bertrand Galpin, Vincent Grolleau, Stefan Umiastowski, Gérard Rio, Laurent Mahéo

Design and application of an instrumented projectile for load measurements during impact

Bertrand Galpin[a], Vincent Grolleau[b,*], Stefan Umiastowski[a], Gérard Rio[b] and Laurent Mahéo[a]

[a] *Centre de recherche des Ecoles de St-Cyr–Coëtquidan (CREC St-Cyr) Ecoles Militaires de Coëtquidan, 56381 GUER cedex, France;*
[b] *Laboratoire de Génie Mécanique et Matériaux (LG2M), Université de Bretagne Sud, BP 92116, rue Saint Maudé, Lorient, France*

No standardised device is available yet to measure contact forces continuously during transverse impacts caused by a projectile on a metal plate or a thin-walled structure. This study describes the design and validation phases of an instrumented projectile (mass = 1 kg) that can be used to achieve such measurements. The impact force, indeed, is computed from the strain data collected by some strain gauges glued on to a projectile part, which remains elastic during shock. Under numerically defined conditions, the projectile geometry makes it possible to record signals that are not disturbed by the reflections of the compressive and tensile strength waves appearing inside the projectile during and after shock. Gauge signal post-filtering is then virtually useless. The strain gauge-instrumented projectile sensitivity is used to study the effects of small clamping pressure variations during the transverse impact study on shipbuilding steel plates. A second application deals with the impact of an automotive steel dome initially drawn with a bulge test apparatus.

Keywords: dome; impact; instrumented projectile; contact force; crash

Notation

C :	sound celerity
e:	relative error
F_b :	resultant load on a section of the bar
F_i :	applied load
F_p :	resultant load on a section of the projectile
F_{pc} :	corrected load measured by the projectile
T :	rising time of the load

1. Introduction

Shipbuilding, car and plane manufacturers, among others, need some dynamic test characterisations to identify the behaviour law parameters of the materials they use. Other dynamic tests are used to study the performances of the whole structure (crash test in the car industry, for instance). However, when the dimensions of the structure do not allow for such tests, conducting dynamic tests on part of the structure only [11,21,25,32] or resorting to scaling laws [14,26] is possible. Whatever the experimental method used [8] (falling weights [4,9,16,20,28], Hopkinson bars [17,29–31], propelled projectiles [12,14,24]), the objective of the tests is the collection of continuous data on contact force evolution in time to validate the analytical solutions [12,20,24] or adjust the numerical simulations [15].

The strain gauge-instrumented projectile described here has been developed to meet these requirements. Several instrumented projectiles with characteristics very similar to what is required here are found in the literature [4,9,16] (mass of approximately 1 kg and energy at work of the order of $\geq$100 J [12,15,20,28]). The instrumentation consists of either piezoelectric accelerometers or strain gauges. Knapp et al. [18] have described the use of these measuring systems for impact devices. The post-filtering of all the signals generated here, however, is absolutely necessary to reduce the influence of the elastic wave reflections propagating inside the projectile [19].

Tanimura et al. [3,22,23], on the other hand, has developed a specific impact force measurement device, called the sensing block system (SBS) (Figure 1). The sensor is a 70-kg steel mass comprising two cylindrical parts fixed on the frame of a rapid tensile testing machine. The impact load, F_i, is applied to the tip of the sensing projection (SP) (diameter d= 15 mm, height h= 20 mm), in the middle of which the strain gauges are glued. The base block (BB) attached to the SP is larger (diameter H= 200 mm, height D= 300 mm). Tanimura et al. [23] has demonstrated that, for a rising time T of the applied load F_i, measurement errors are directly connected to the SP dimensions h and d. He also proved that the selected SP dimensions particularly suit the creation of a very quick uniform strain state around the strain gauges essential for the calculation of the resultant force F_p within the SP section. Consequently, the SBS can be used to achieve F_i measurements with an error less than 3% and no signal filtering providing that T remains always higher than 25 μs.

*Corresponding author. Email: vincent.grolleau@univ-ubs.fr

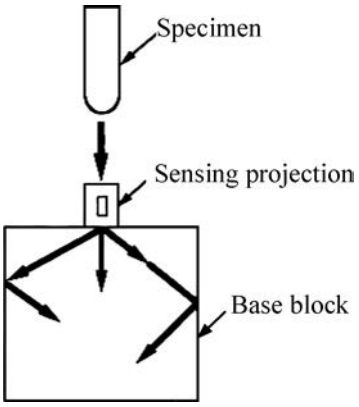

Figure 1. Schematic of the Sensing Block System proposed by Tanimura (extracted from [2]).

This article initially presents the design of a 1-kg maximum strain gauge-instrumented projectile, founded on Tanimura's principle, to measure the forces applied to thin-walled structures during impact tests conducted at a velocity of 20 m/s. Firstly, the experimental device is described, followed by a numerical study to examine the sensitivity to load rising time. Secondly, the experimental validation based on the Hopkinson bar method is discussed. Finally, two applications are presented: first, in which the projectile sensitivity is used to show the effects of very small clamping pressure variations on a shipbuilding steel plate during a transverse impact, and second, concerning the impact of a dome obtained from a hydraulic bulge test on an automotive steel sheet.

2. Experimental device

The experimental device consists of a crossbow propelling the projectile straight down with an available kinetic energy of approximately 100 J (Figure 2). The tests are carried out on steel specimens for use in the shipbuilding industry and held in position by jaws clamped tight by two hydraulic jacks applying a 120-kN pressure each. The dimensions of the plates include 224-mm length between the jaws, 15-mm width and 4-mm thickness. Two strain gauges are glued on the lower and upper faces of the specimen, 50 mm away for the centre (impacted point). A non-contact displacement transducer (Bullier int. M5L/100) placed under the specimen indicates the vertical displacement of the sheet's lowest point within the impacted area.

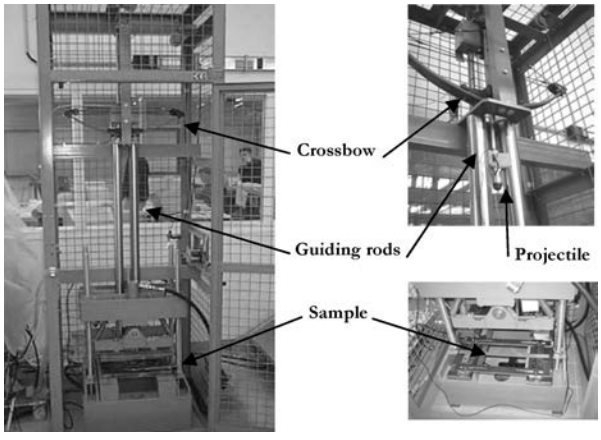

Figure 2. The impact device.

Description of the projectile

The projectile consists of an SP attached to a BB just as in the case of Tanimura's device. The SP dimensions are also as those proposed by Tanimura. The BB dimensions depend on the device guiding system and the total projectile mass, which should not exceed more than 1 kg so as to fall at velocities around 20 m/s. Thus, the only independent geometrical parameter is the diameter D of BB. A 550-mm high and 10-mm diameter aluminium rod is use to drive the projectile downward with the crossbow (Figure 3).

Projectile sensitivity to rising time

To study the effect of the load rising time, T, on the experimental projectile response, a parametric numerical simulation is carried out. The results are then compared with the result of Tanimura et al. [23]. From the sensitivity analysis of the response to the meshing (Figure 4) , the dimension of the SP mesh is 1.5 mm $\times$ 1.5 mm $\times$ 2 mm. The projectile is made of a 42CrMo4-hardened steel with an elastic limit of 800 MPa. The projectile behaviour is governed by a linear elasticity law with a Young's modulus E= 210,000 N/mm^2 and a Poisson's ratio $\nu = 0.3$.

The projectile response, for different rising times T, is obtained from the deformations observed on a 6-mm surface (gauge length) whose centre is located 12 mm away from the F_i application point (Figures 5 and 6) . Under the assumptions of elasticity and strain homogeneity, the load F_p exerted on the straight section of the SP at the level of the gauges can be calculated using Hooke's law. Assuming a rigid solid, Langseth [12] established the relationship between F_p and the corrected impact force F_{pc} as

$$F_{pc} = F_p \left(1 + \frac{M_n}{M - M_n}\right) = a F_p, \qquad (1)$$

where M_n is the mass of SP between the impact point and the gauges and M is the total mass of the projectile. Coefficient a= 1.016, a value which is applicable for all the results presented here.

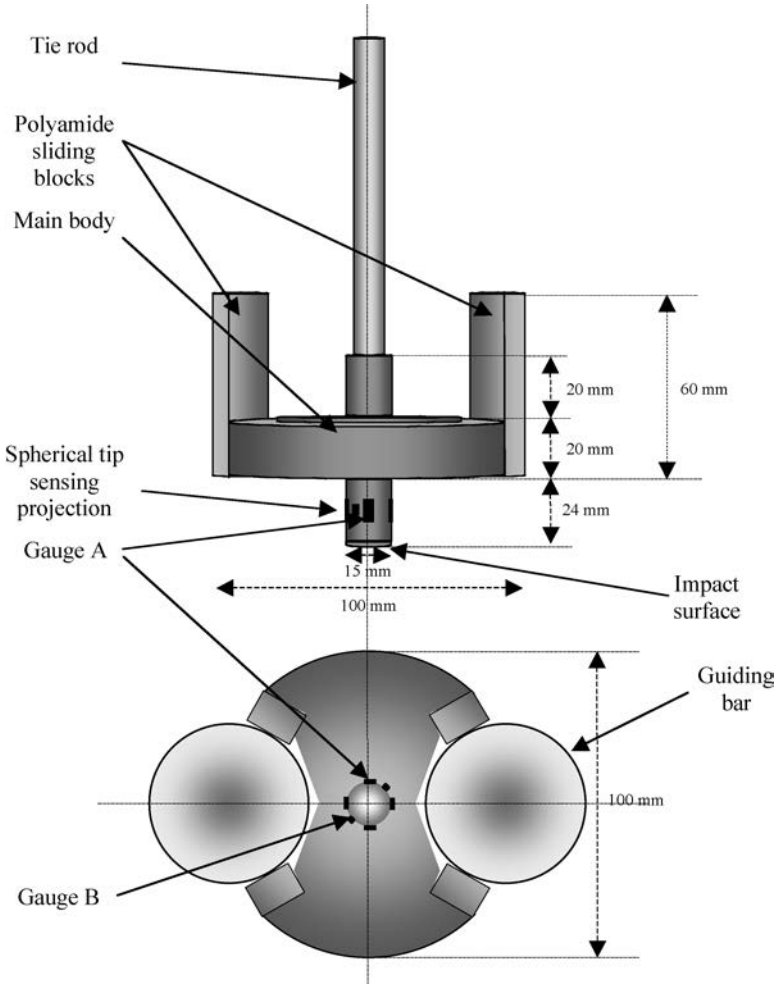

Figure 3. Projectile schematic diagram.

The two parameters, amplitude A and rising time T, of the load versus time evolution are given in Figure 5. Considering the linear elasticity of the material and the small perturbation hypothesis (small strains and small displacements), the two parameters of the relative error e study are the rising time T and the ratio of the diameters D/d. The

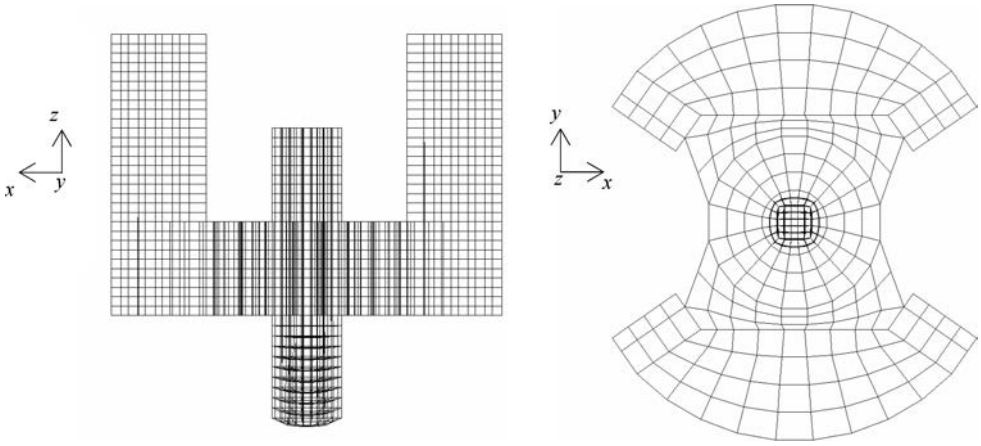

Figure 4. Projectile meshing.

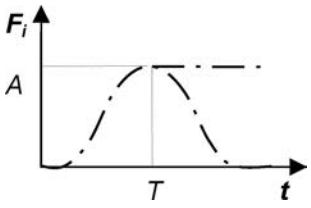

Figure 5. Load F_i applied to sensing projection. $F_i = A\{1 - \cos(\pi t/T)\}/2$, for $t < T$; $F_i = A$, for $t \geq T$.

relative error, e (Equation (2)), decreases with the ratio D/d if $D/d < 2.0$ and remains constant for $D/d > 2.0$. Figure 3 presents the actual geometry of the projectile. The projectile mass is 960 g.

$$e = (F_{pc} - A)_{\max} / A \tag{2}$$

The results for error e versus rising time T are as follows: 25% for 15 μs; 13.8% for 20 μs; 7.4% for 25 μs; 3.7% for 30 μs; 2.7% for 40 μs; 1.9% for 50 μs; and 0.9% for 80 μs. In comparison, Tanimura's SBS shows an error of approximately 3% for a loading time of 25 μs. If this 3% threshold is determined as the optimum performance for the strain gauge-instrumented projectile, the load signal rising time must be higher than 35 μs.

3. Experimental validation

Projectile instrumentation

For transient measuring, the minimum measurable wavelength is determined by the gauge length L. A recommended maximum value of L is given by $L < CT/10$, where C is the sound celerity under uniaxial stress conditions and T is the period of the signal [1]. For a minimum period $T =$ 15 μs and a steel sound celerity $C =$ 5172 m/s, the maximum recommended gauge length is 7.5 mm. Six strain gauges are mounted vertically halfway up the SP:

- Four type A gauges (Vishay CEA-06-250UN-120, gate length = 6.35 mm) placed at 90° to each other.
- Two type B gauges (Kyowa KFG-2-120-C1-11, gate length = 2 mm) placed diametrically opposite and arranged between two type A gauges (Figure 3).

Each pair of diametrically opposite mounted gauges is embedded in a half tensile bridge circuit so as to filter possible flexional strains. The signal is amplified using a high frequency A2 Vishay controller and recorded with data acquisition board (1-MHz sampling and 12-bit digitising). As the signals achieved using gauges A and B are nearly identical, we can conclude that type A gauge length is low enough for the measurements carried out here. Consequently, all the measurements discussed below come from the four type A gauges only.

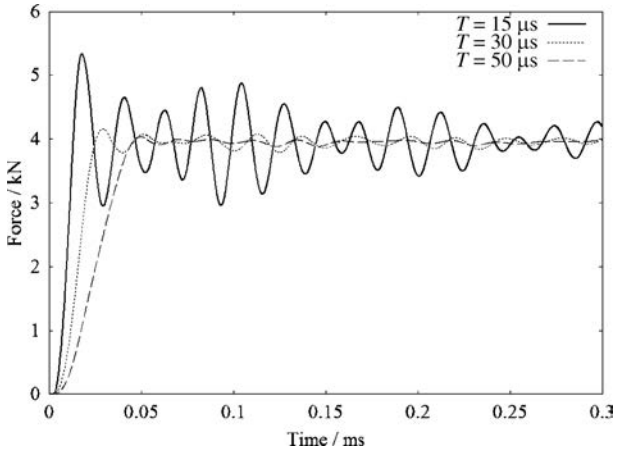

Figure 6. Projectile response to type F_i loading (T varying from 15 to 50 μs).

Experiment

A compression test of the projectile using a universal testing machine is carried out for the quasi-static calibration of the load value computed from the projectile strain measurements. The dynamic validation of the projectile (Figure 7) is carried out by making an impact on one end of a 390-mm long cylindrical bar (Figure 8) whose diameter is identical to that of SP (15 mm). The bar is equipped with type A strain gauges glued axially 50 mm away from the impacted end to comply with St. Venant principle (Figure 9).

The bar, which can be considered as a Hopkinson bar, is supported by a 200-mm diameter and 50-mm high cylindrical element, and the wave initiated at the point of impact at the initial shock time travels the 390-mm free length of the bar before being partially reflected because of the sudden change in section from the upper surface of the support . The wave then covers 340 mm before reaching the gauges again. As the wave velocity C is 5172 m/s, no wave reflection interferes with the gauge signals before the first 139-μs

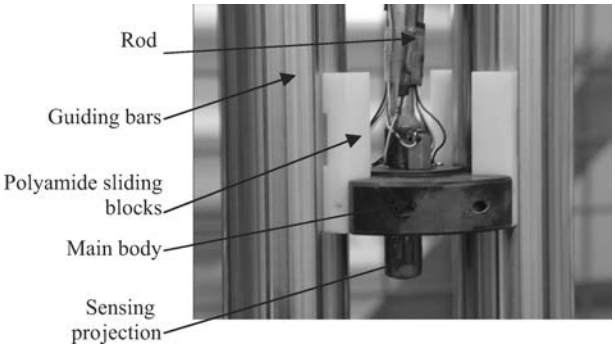

Figure 7. The instrumented projectile.

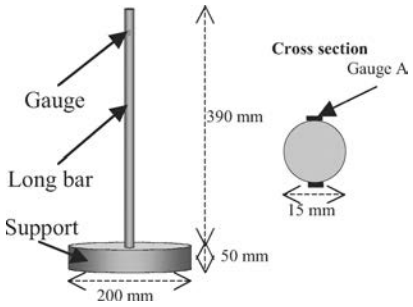

Figure 8. Validation bar.

after the shock. Force F_b, comparable with the projectile, is deduced from the elongation strain. So, both F_p and F_b can be easily compared. Figure 10 presents the results of tests performed at 2.39 m/s. A 7.7-μs time shift is necessary for the bar signal because the gauges are not glued at the identical distance from the impacted tips (10 mm for the projectile gauge and 50 mm for the bar gauge).

The strong similarity between both projectile and bar gauge signals observed during 139 μs with a maximum error of 4% confirms the experimental validity of the measuring system principle, that is, the combination of a sensor in dynamic equilibrium (the SP) with a massive device (the BB).

4. Applications

Transverse impacts on rectangular samples

The instrumented projectile is used for transverse impact tests on flat rectangular specimens held in position by the clamping mechanism presented in the 'Experimental device' section.

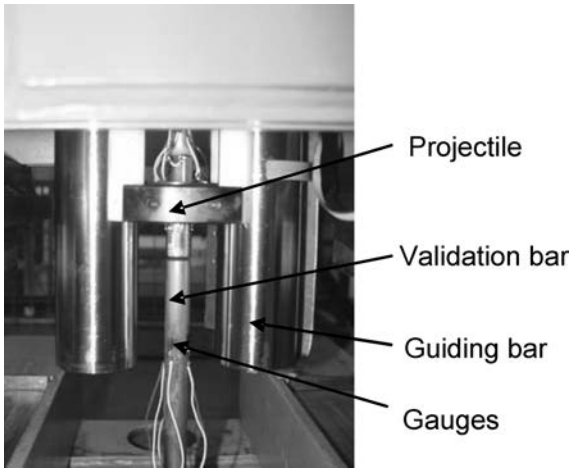

Figure 9. Projectile and validation bar.

To address the repeatability of impact force measurements, four different impact tests on steel plates (E355) for use in the shipbuilding industry are carried out. The impact velocity is 10.3 m/s. The clamping pressure is 128 MPa. For this series of tests, the specimen tips outside the jaws are pinned to the frame to avoid any sliding of the plate between the jaws. Figure 11 presents the four load signals achieved in the defined conditions. Some high-frequency oscillations are observed approximately 1 ms after the impact. The rising times are 20 μs. This value proves a little short for the optimum performances of the projectile as observed in the numerical study.

After 1 ms, the oscillation frequency sharply decreases and justifies the use of the instrumented projectile for impact force measurements. The strain gauges on the upper and lower faces of the specimen 50 mm away from the impact point reveal that the specimen undergoes some plastic deformations, which may account for the oscillation attenuation. Therefore, the determination of the repeatability mean standard deviation really starts after 1 ms. The measurement standard deviation is calculated for all measurements throughout the four tests. The maximum and averaged mean standard deviations after 1 ms are σ_{maxi}= 0.1 kN and $\sigma\sigma_{\text{ave}}$= 0.04 kN, respectively.

Two tests are carried out at clamping pressures of 128 and 138 MPa, respectively, that is, a difference of 6%. The repeatability error of the measurements obtained with the laser displacement transducer or with the accelerometer placed in the projectile head [10] is not small enough to conclude that the difference is significant. Yet, the signal coming from the gauges glued on to the specimen changes significantly. Figure 12 displays the contact forces achieved here with the instrumented projectile. The maximum and mean load deviations after 1 ms are E_{maxi}= 0.47 kN and E_{ave}= 0.14 kN, respectively. The maximum deviation observed between both curves is three times higher than the maximum standard deviation achieved during the repeatability tests for the same period. The projectile proves sensitive enough to account significantly for the impact force history for a 6% variation in the clamping pressure. The strain gauge-instrumented projectile, therefore, can be used to achieve a new experimental validation observable in a more sensitive way than what used to be measured during transverse impact tests on steel plates until now.

Crushing of spherical domes

For this second application, experimental and simulated stress results for an impact test on a steel dome are compared. The spherical dome is obtained by performing a quasi-static bulge test on an automotive steel sheet fixed on the peripheral support of a circular orifice. Both plate and bulging system geometries are given in Figure 13.

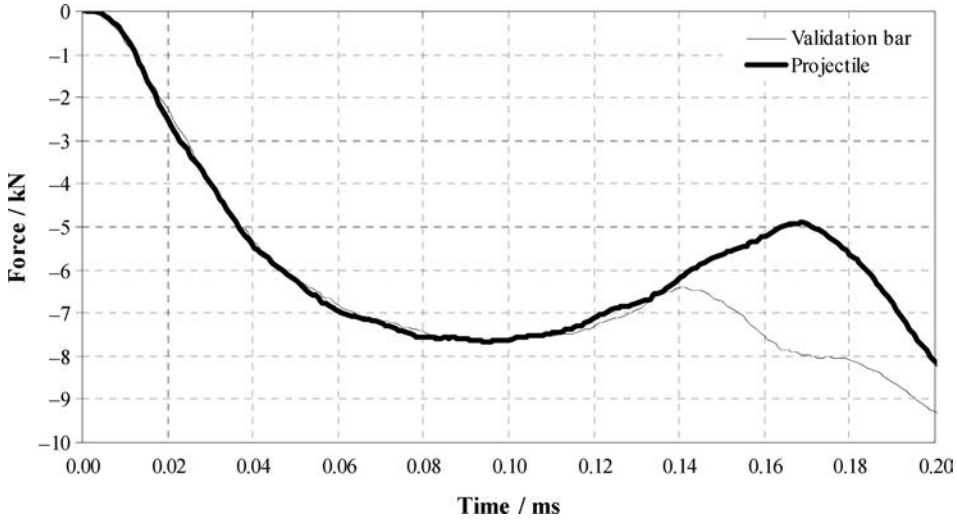

Figure 10. Projectile test on the validation bar.

The material behaviour is modelled using the three parameters law (BARLAT_3_PARAMETER) proposed by Barlat and Lian [2] for modelling sheets with anisotropic materials under plane stress conditions. The behaviour law coefficients are as given in reference [27]. Equation (3) gives the equation for flow stress, where σ is the yield stress in MPa and ε_p the effective logarithmic plastic strain. The Barlat's yield surface parameter, $m = 2$, is equivalent to the use of the Hill48 criterion. Lankfort's coefficients are $r_{00} = 2.16$, $r_{45} = 1.611$ and $r_{90} = 2.665$, respectively. The strain rate sensitivity is assumed to be negligible during impact. The mesh is composed of Belytschko Lin Tsay's shell elements with seven through thickness integration points. The projectile model is presented in the 'Projectile sensitivity to rising time' section. The contact used for the impact is CONTACT_AUTOMATIC_GENERAL [18].

$$\sigma = 544(0.0088 + \varepsilon_p)^{0.27}. \tag{3}$$

The numerical simulation is performed in two steps:

- First, dome bulging is simulated. Final bulging pressure is 5.2 MPa. The comparative chart given in Table 1 displays the main characteristic quantities for comparing the computed and measured units of the dome (deflection, apex thickness and radius). The experimental and numerical results satisfactorily agree with regard to this phase.

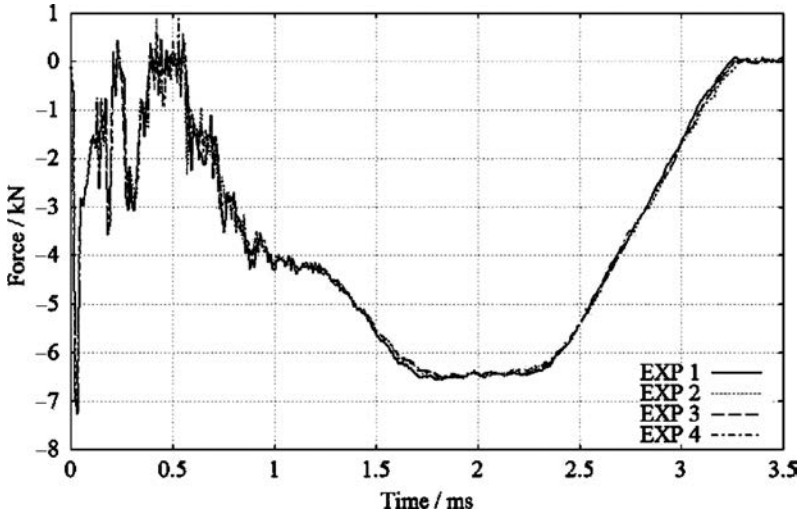

Figure 11. Test repeatability at a 128.1-MPa clamping pressure.

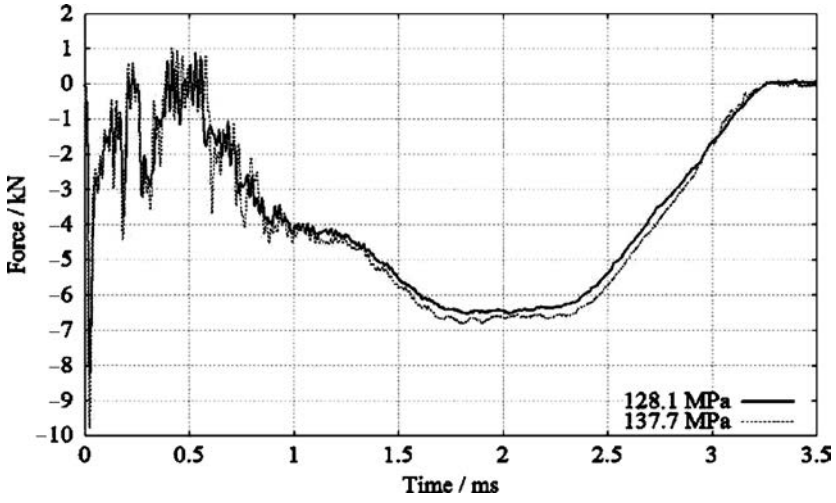

Figure 12. Projectile sensitivity to clamping pressure.

- Second, the impact on the dome is simulated. The impact velocity is 12.4 m/s. Figure 14 shows the projectile and spherical dome meshing. Simulated and experimental stress curve plots are given in Figure 15. The simulated curve is computed from the average of the strains of the elements corresponding to the location of gauges on the projectile. Both curves, therefore, are obtained by using the same procedure for the force calculation from the strain measurements on the projectile.

Both curves satisfactorily agree up to 3.7 ms, a value that corresponds to the moment the plate begins to spring back. This observation agrees with the literature, in which specific numerical precautions, not considered here, to simulate springback accurately are recommended [5]. The maximum stress value is correctly simulated with a mean error of 3% in comparison with the experimental signal. The force signal oscillations, which are observed during the impact tests in the 'Transverse impacts on rectangular samples' section and because of the incident force rising time and the elastic behaviour of the plate at the beginning of the tests, disappear. Crushing of spherical domes, indeed, disappears due to the formation of rolling plastic hinges [6,7]. The impact is all the more enhanced because of the small projectile diameter and thin plate size.

Table 1. Comparison of experimental and numerical results.

	Deflection f (mm)	Apex thickness t_a (mm)	Apex radius R_d (mm)
Computed units	67.2	0.68	151
Measured units	68	0.69	155

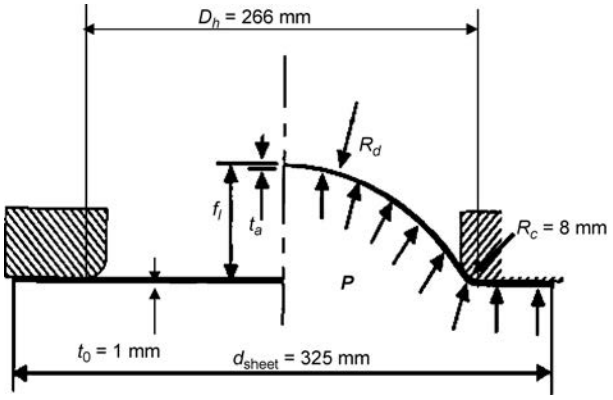

Figure 13. Plate and bulging system geometry.

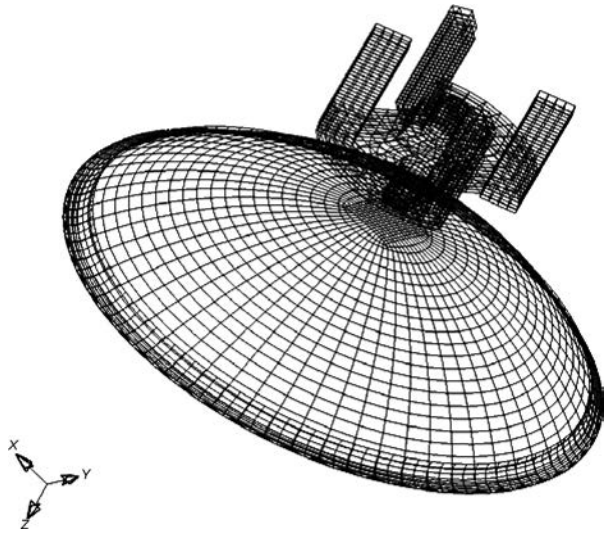

Figure 14. Projectile and spherical dome meshing.

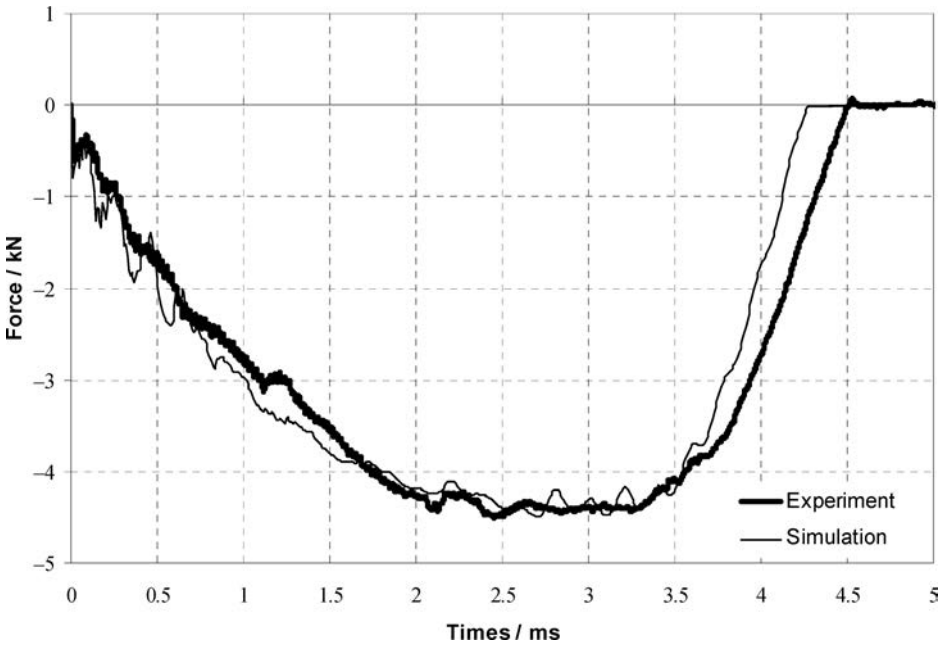

Figure 15. Simulated and experimental load curves.

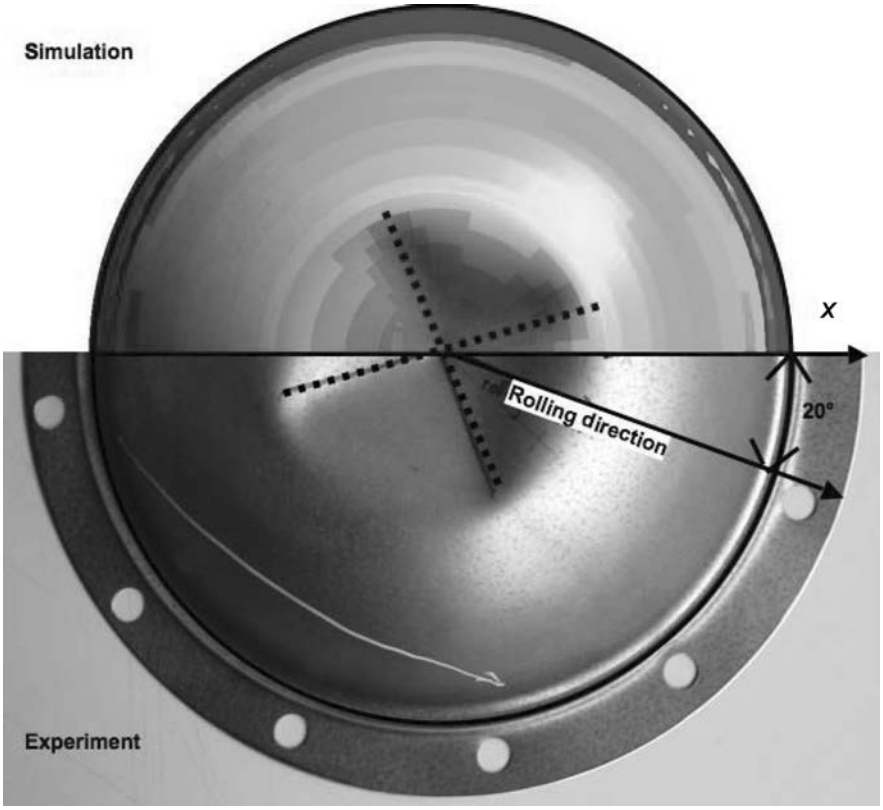

Figure 16. Experimental and simulated orientation of the wrinkles of the impacted bulge.

The impacted point displacements are also compared. A 3.3% error on the maximum displacement and a 4.3% error on the final displacement after springback are observed. Figure 16 shows that the number and the orientation of both the simulated and the experimental wrinkles agree satisfactorily. The anisotropic feature of the material causes wrinkling, whereas wrinkle orientation is independent of the meshing used. The simulated wrinkles, given in the figure, depend on the material anisotropic directions, which present a 20° shift in relation to the meshing axes of symmetry. No wrinkle appears if an isotropic law is used for the simulation.

The results demonstrate the relevance of the instrumented projectile for the validation of numerical simulations to study the impacts on a drawn structure by comparing experimental and simulated impact loads.

5. Conclusions

This article reports on a strain gauge-instrumented projectile used to carry out force measurements during impact tests on steel plates.

From the ensuing bibliographic study, a compact 960-g projectile is developed on the basis of Tanimura's SBS. To avoid filtering of the force signal sent by the projectile, its geometry has been especially studied to prevent interferences of elastic wave reflections during strain measurements. The numerical study reveals the sensitivity of the load rising time. Rising time, therefore, must be higher than 35 μs for the relative error from the sensor projectile to remain below 3% whatever the D value if $D/d > 2.0$.

Tests on 4-mm thick steel plates for use in the shipbuilding industry have been carried out using the sensor projectile. The results make it possible to validate the projectile optimum operating condition regarding the rising time of the applied load. For rising times of more than 35 μs, the mean standard deviation is 0.04 kN for a maximum force of 6.5 kN. This characteristic is used to prove that a 6% clamping pressure variation on the specimen causes a significant variation of the maximum stress value when the specimen is fully plastified. This difference in the experimental conditions is also validated by the strain gauges glued on to the specimen. These results are obtained in spite of the sensitivity of the displacement transducers that does not make it possible to show significant measurement changes. This confirms the relevance and sensitivity of the new projectile presented.

Finally, impact measurements on a drawn steel dome achieved through bulging are used to validate the numerical simulation throughout the impact duration. Consequently, the validation of impact numerical studies on bulges using new experimental measurements of the impact load is now possible.

Acknowledgment

The authors thank the Conseil Régional de Bretagne for their support of this study through grant 'De la mise en forme au comportement dynamique, G2RB2M.' The authors are also grateful to Mr. H. Bellegou and Mr. F. Portanguen from UBS University for technical assistance.

References

[1] J. Avril, *Encyclopédie d'analyse des contraintes*, Micromesures, Malakoff, 1984.

[2] F. Barlat and J. Lian, *Plastic behavior and strechability of sheet metals – part 1. A yield function for orthotropic sheets under plane stress conditions*, Int. J. Plasticity. 5 (1989), pp. 51–66.

[3] Y. Chuman et al., *A sensing block method for measuring impact force generated at a contact part*, Int. J. Impact Eng. 19 (1996), pp. 165–174.

[4] G.A.O. Davies and X. Zhang, *Impact damage prediction in carbon composite structures*, Int. J. Impact Eng. 16 (1995), pp. 149–170.

[5] M.Y. Demeri, M. Lou, and M.J. Saran, *A benchmark test for spring back simulation sheet metal*, Soc. Automotive Eng. (2000), paper 200-01-2657, International Body Engineering Conference and Exposition, Detroit, MI, October 2000.

[6] J.G. de Oliviera and T. Wierzbicki, *Crushing analysis of rotationally symmetric plastic shells*, J. Strain Anal. 17 (1982), pp. 229–236.

[7] G.L. Easwara Prasad and N.K. Gupta, *An experimental study of deformation modes of domes and large-angled frusta at different rates of compression*, Int. J. Impact Eng., 32 (2005), pp. 400–415.

[8] J.E. Field et al., *Review of experimental techniques for high rate deformation and shock studies*, Int. J. Impact Eng. 30 (2004), pp. 725–775.

[9] P.B. Gning et al., *Damage development in thick composite tubes under impact loading and influence on implosion pressure: experimental observations*, J Composites. 36 (2005), pp. 306–318.

[10] V. Grolleau, G. Rio, and S. Maillard, *Impact of thin plates with losses of contact*, 4th Int. Symp. *Impact Engineering*, Japan, Elsevier Sciences, 2001.

[11] Z.Q. Huang, Z.Q. Chen, and W.T. Zhang, *Pseudo-shakedown in the collision mechanics of ships*, Int. J. Impact Eng. 24 (2000), pp. 19–31.

[12] O. Jensen, M. Langseth, and O.S. Hopperstad, *Experimental investigations on the behaviour of short to long square aluminium tubes subjected to axial loading*, Int. J. Impact Eng. 30 (2004), pp. 973–1003.

[13] J. Knapp et al., *Measurement of shock events by means of strain gauges and accelerometers*, Measurement 24 (1998), pp. 87–96.

[14] M. Langseth and P.K. Larsen, *Dropped objects plugging capacity of steel plates: an experimental investigation*, Int. J. Impact Eng. 9 (1990), pp. 289–316.

[15] M. Langseth, O.S. Hopperstad, and A.G. Hanssen, *Crash behaviour of thin-walled aluminium members*, Thin-Walled Struct. 32 (1998), pp. 127–150.

[16] J.M. Lifshitz, F. Gov, and M. Gandelsman, *Instrumented low-velocity impact of CFRP beams*, Int. J. Impact Eng. 16 (1995), pp. 201–215.

[17] K. Liu et al., *Dynamic behaviour of ring systems subjected to pulse loading*, Int. J. Impact Eng. 31 (2005), pp. 1209–1222.

[18] Ls-Dyna, *Keyword User's Manual*, Livermore Software Technology Corporation, Livermore, 1999.

[19] S. Sahraoui and J.L. Lataillade, *Analysis of load oscillations in instrumented impact testing*, Eng. Fract. Mech. 60 (1998), pp. 437–446.

[20] W.Q. Shen et al., *An experimental investigation on the failure of rectangular plate under wedge impact*, Int. J. Impact Eng. 28 (2003), pp. 315–330.

[21] B.C. Simonsen, *Ship grounding on rock – part II. Validation and application*, Marine Struct. 10 (1998), pp. 563–584.

[22] S. Tanimura, *A new method for measuring impulsive force at contact parts*, Exp. Mech. 24 (1984), pp. 271–276. .

[23] S. Tanimura et al., *Evaluation of accuracy in measurement of dynamic load by using load sensing block method*, Proceedings of 4th International Symposium on Impact Engineering ISIE4 (2001), pp. 77–82, Kumamoto, Japan.

[24] S.P. Virostek, J. Dual, and W. Goldsmith, *Direct force measurement in normal and oblique impact of plates projectiles*, Int. J. Impact Eng. 6 (1987), pp. 247–269.

[25] G. Wang, K. Arita, and D. Liu, *Behavior of a double hull in a variety of stranding or collision scenarios*, Marine Strucut. 13 (2000), pp. 147–187.

[26] H.-M. Wen and N. Jones, *Experimental investigation of the scaling laws for metal plates struck by large masses*, Int. J. Impact Eng. 13 (1993), pp. 485–505.

[27] D.-Y. Yang et al., *Numisheet 2002*, proc. 5th Int. Conf. and Workshop, Numerical Simulation of 3D Sheet Forming Processes, Jeju Island, Korea, 2002.

[28] M. Zeinoddini, G.A.R. Parke, and J.E. Harding, *Axially preloaded steel tubes subjected to lateral impacts: an experimental study*, Int. J. Impact Eng. 27 (2002), pp. 669–690.

[29] H. Zhao and S. Abdennadher, *On the strength enhancement under impact loading of square tubes made from rate insensitive metals*, Int. J. Solids Struct. 41 (2004), pp. 6677–6697.

[30] H. Zhao and G. Gary, *Crushing behaviour of aluminium honeycombs under impact loading*, Int. J. Impact Eng. 21 (1998), pp. 827–836.

[31] H. Zhao, S. Abdennadher, and R. Othman, *An experimental study of square tube crushing under impact loading using a modified large scale SHPB*, Int. J. Impact Eng. 32 (2006), pp. 1174–1189.

[32] L. Zhu and D. Faulkner, *Damage estimate for plating of ships and platforms under repeated impacts*, Marine Struct. 9 (1996), pp. 697–720.